Grid Laser Marking Influence on High-Strength Steels Tensile Test Behavior

German Abate
Instituto Nacional de Tecnologia Industrial

Alejandro Simoncelli
Instituto Nacional de Tecnologia Industrial

Nazareno Antunez
Instituto Nacional de Tecnologia Industrial

Vitaliy Martynenko
Instituto Nacional de Tecnologia Industrial

INFLUENCIA DEL GRILLADO LÁSER SOBRE EL COMPORTAMIENTO DE PROBETAS DE TRACCIÓN DE UN ACERO DE ALTA RESISTENCIA

GRID LASER MARKING INFLUENCE ON HIGH-STRENGTH STEELS TENSILE TEST BEHAVIOR

Daniel Martinez Krahmer[1,2], Germán Abate[1,2], Alejandro Simoncelli[1,2], Nazareno Antunez[1,2], Vitaliy Martynenko[1,2], Daniela Perez[1,2], Norberto López de Lacalle[3,4]

[1] Centro de Investigación y Desarrollo en Mecánica, Instituto Nacional de Tecnología Industrial (INTI), Avenida General Paz 5445, 1650, Miguelete, Provincia de Buenos Aires, Argentina

[2] Facultad de Ingeniería, Universidad Nacional de Lomas de Zamora, Juan XXIII y Camino de Cintura, 1832, Buenos Aires, Argentina

[3] Aeronautics Advanced Manufacturing Center CFAA, E48170 Zamudio, Spain

[4] Department of Mechanical Engineering, University of the Basque Country (UPV/EHU), E48013 Bilbao, Spain

dmartinez@inti.gob.ar

Recibido: 23/07/20 – Revisado: 21/09/20 -- Aceptado: 14/10/20 - DOI: A cumplimentar por el Editor

ABSTRACT:

Automotive car companies are using AHSS (advanced high strength steels) over the last 20 years to reduce vehicle weight and improve safety. The new steels can achieve higher strength and good fatigue resistance, but some issues related to springback and low formability are also a big concern. Thus, companies need to extend their know-how regarding material behaviour, design rules and manufacturing processes.

Therefore, materials characterization laboratories are working to obtain the new formability charts of the steels. The grid laser marking of test pieces is a recent approach. However, the marking process must accomplish three main aspects: indelibility during the tensile testing procedure, precision, and of course, it must not affect the mechanical properties of studied steels.

This work is focused on the laser marking of test pieces using a Ytterbium fiber laser. A dual phase steel (type JFE CA 1180) is studied. Process parameters are defined.

Keywords: grid marking, laser, advanced high-strength steels, AHSS, formability diagrams, mechanical properties

1.- INTRODUCTION

The automotive sector is a prime consumer of stamped sheet metal parts [1]. For some years now, the replacement of white-body parts stamped on conventional steels, with high-strength steels (for example dual phase steels) is continuous. In 1998, the car company SAAB introduced for the first time a hot stamped part, the four door reinforcements (Side Impact Beams). AHSS (Advanced High-Strength Steels) steels allow for thinner, lighter parts, with enhanced mechanical properties in the body structure [2]–[3]. These steels are a large family that includes so-called dual-phase, ferritic-bainitic, martensitic, etc. [4], characterized by their increased mechanical strength.

Given the continuous and spreading use of these new steels, traditional stamping companies must reconvert their know-how since high-strength sheets present a very different plastic behavior, which is why they require stamping dies design with more knowledge about sprinback and sheet plastic behavior [5]–[6]. Differences in behavior make these very difficult materials to deform, with more significant elastic recovery that causes greater loads on both the stamping tools and press machines [7].

To facilitate the forming of these steels, the hot stamping technique is used [8]-[9], and even in small-size batches, with a single forming tool [10], or using two of them to achieve better part geometric accuracy [11]. Thus, industrial hot stamping systems improve in design and effectiveness with each new automotive program [12].

The practical way to know the behavior of sheet metal versus deformation during stamping is by obtaining the forming limit diagrams [13]. This activity requires tensile testing [14], for the left part of the diagram where the deformations are of tension-compression type and Nakazima for the right part, where the deformations are tension-tension [15]. After obtaining the limit diagrams, they can be used in the stamping simulation software, to adjust dies design, reaching parts with enough accuracy in high strength steels [16].

As both in tensile and Nakazima tests it is necessary to deform the specimens until final breakage, in order to measure the evolution of deformations during forming, test specimens must be marked with a circular grided pattern. The grids are measured optically just before and after test, so that the deformation reached in the areas surrounding the breakage can be established, and so the obtained deformation values are turned to the limit diagram. These grids must be made using an indelible method [17] and precise enough [18], not affecting locally the steel properties [19]. One process that meets these three aspects can be laser engraving [20]. Specifically, S. Guk and his collaborators [19], worked on a dual phase steel, focusing on the relationship between laser grid marking and steel conformability, according to Erichsen test. These alterations were characterized by a notch factor. As a result of the tests, they found that formability decreased as the notch factor increases. However, they did not extend their studies to tensile testing.

This work proposed the operating conditions of a nanopulsed Yterbio fiber laser, to performing a grid-shape marking easily readable; the so produced grid does not affect the mechanical properties of tensile specimens of high-strength steel of the type JFE CA 1180, when comparing grid laser marking and non-grid laser marking samples used as a reference.

2.- MATERIALS AND METHODS

Working parts are metal sheets, made in high-strength steel, designated as JFE CA 1180; Yield Strength (min.) = 825 N/mm^2; Tensile Strength = 1180 N/mm^2 and Elongation under fracture load = 7 %, 1.2 mm thick. This material was selected for its increased sensitivity to thermal involvement caused by laser grid marking. The nominal chemical composition is presented in Table I:

Element	C	Si	Mn	P	S	Fe
Wt%	0.12	0.50	2.0	0.01	0.003	Balance

Table I: Nominal chemical composition of sheet steel JFE CA 1180

The steel mechanical properties were obtained according to ASTM E8, extracting the tensile specimens along the sheet rolling direction from a single batch. The tensile specimens were cut with a waterjet cutting machine with garnet abrasive 80. The machine was Flow Mach 3 model 1313b, with a dynamic cutting head and 60,000 psi intensifier pump. Feed rate of 700 mm/min was used in cutting. AWJ does not affect borders and prevents from distortion in tensile tests.

The pattern grid on one of the faces of the tensile specimen was a circular pattern of 2.5 mm in diameter, as indicated by ASTM E2218. The grids were made with an Yterbio fiber laser, brand Hans laser with an IPG source model YLPN-1-100-20-M, which wavelength of 1064 nm, maximum power of 20 W, and frequencies adjustable between 20 to 200 kHz. The laser software has the possibility to control 12 variables. However, in previous studies [21]-[22], it was determined that they are the i) focus, (ii) power and (iii) number of passes, the variables that most influence the thermal affectation and readability of engraved marks. The maximum frequency (200 kHz) was also chosen to produce the lowest possible penetration.

Regarding the parameter "Beam displacement speed", it was set to 100 mm/s to obtain accurate and productive engravings, with reduced heat input. The increase of the latter parameter, as well as the decrease of the "Delay to shutdown" produce a similar effect to the decrease "Power". Along with the frequency, travel speed, and delay to shutdown, the remaining variables were fixed on all engravings: Jump speed: 100 mm/s; Opening time: 0.1 s; Advance to laser ignition: 0 s; Delay to movement on a line: 0 s; Jump Delay: 0 s; Stop at the corners: 0 s and Stop at the layer: 1000 s.

On the other hand, tensile tests were carried out on a universal tensile machine Instron Model 5985 of 250 kN capacity, using an Instron 2630-112 brand strain gauge of 50 mm initial length, in order to obtain in each trial the Yield Strength, Tensile Strength, Fracture Strength, Elongation under maximum load, and Elongation under fracture load. Test load application speed was set to 5 mm/min, and tests were carried out in a heated cabin, with temperature and humidity controlled by a TFA model 30 thermohygrometer.

5002 (Temperature was 22ºC and humidity x 40%). Fractographic analyses were done using a Philips SEM 505 Scanning Electron Microscope.

Figure 1 shows the configuration of the test methodology.

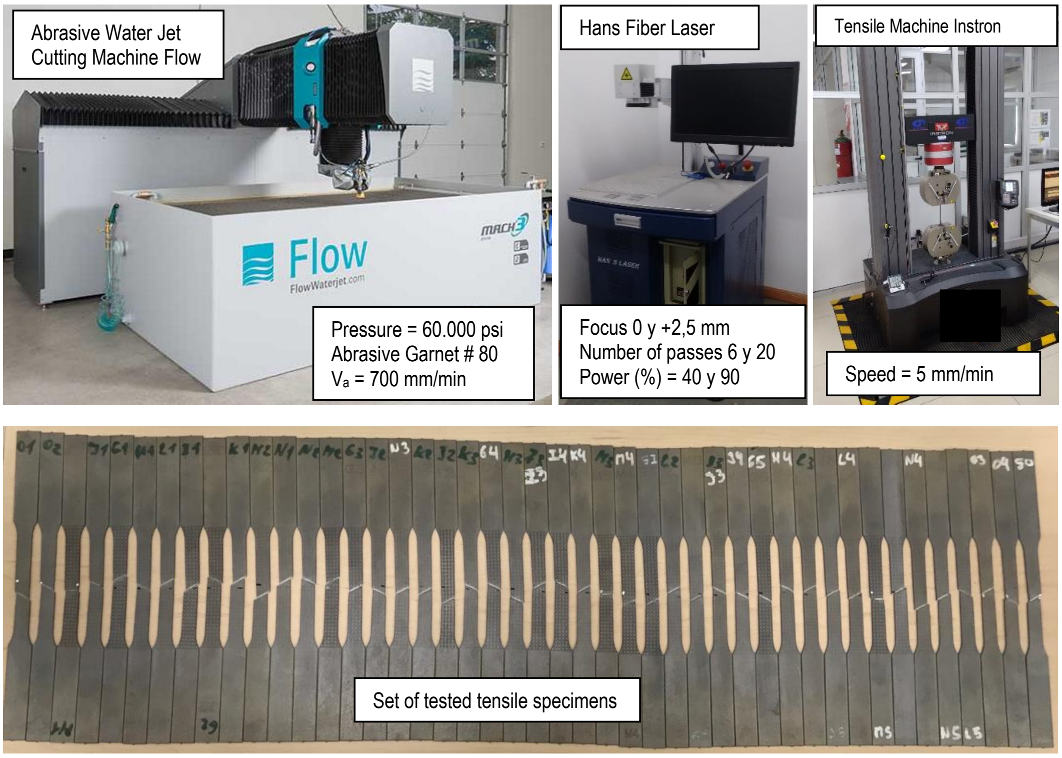

Figure 1: Configuration test methodology (up) and tested specimens (down)

3.- RESULTS

In order to assess the influence of laser engraving variables on the tensile behavior of sheet metal JFE CA 1180 1.2 mm thick, an Experiment Design (DOE) was performed. In principle, it was necessary to define which of the variables involved you want to compare (factors), as well as the range of values they can adopt (levels). Therefore, based on previous experiences [21]-[22], 3 factors were selected with 2 levels each, as shown in Table II.

Factor	Level	Process	Response
Power (Po)	40% and 90%	Tensile test	Yield Strength
Passes (Pa)	5 and 20		Tensile Strength and Elongation under maximum load
Focus (F)	0 and +2.5 mm		Fracture Strength and Elongation under fracture load

Table II: Factors and Levels Used for DOE

To carry out all of the combinations comprised by the three factors with their two levels, it was necessary to perform a total of 8 tensile tests (Number of levels $^{\text{Number of factors}}$ was 2^3).

Appropriate number of repetitions were performed, to determine the amount required so that data populations can be distinguished from the difference to appreciate. For this particular case, the estimated conditions, from previous experiences, were as follows: Number of levels = 2; Maximum difference between the means = 20 MPa ; standard deviation = 8 MPa and power of test = 0.9. These values establish that 5 repetitions are sufficient for research purposes. As with the 8 engraving conditions, they must be added the reference condition (ungraved). Then, the total number of specimens tested was 45 that result of multiplying 9 engraving conditions by 5 repetitions.

For the execution of the tests, 45 abrasive waterjet tensile specimens were cut, corresponding to sheet plates JFE CA 1180 1.2 mm thick. Subsequently, 40 of the specimens were laser-gridded on one of their faces with 8 different strategies (see table III), whereas each group of specimens, made up of each engraving strategy, was identified with a letter starting with the G and ending at N (each letter was accompanied by a number, starting at 1 and ending at 5). Finally, the remaining five specimens were not grided and designated with the letter O. Geometric conditions of the samples were in accordance with ISO ASTM E8.

Table III presents the factorial design of experiments to analyze the influence of three laser operating variables:

Parameters	Specimens								
	G	H	I	J	K	L	M	N	O
Focus (mm)	+2.5	+2.5	+2.5	+2.5	0	0	0	0	Without Grid
Number of passes	5	20	20	5	5	20	20	5	
Power (%)	90	40	90	40	90	40	90	40	

Table III: Grid laser marking conditions for specimens obtained from sheet metals JFE CA 1180 – 1.2 mm

The values obtained during the tensile tests are given in Table IV.

Sample designation	Yield Strength (MPa)	Fracture Strength	Tensile Strength (MPa)	Elongation under maximum load	Elongation under fracture load
G1	984.7	985.4	1239.9	6.1	10.0
G2	993.6	963.5	1253.7	5.6	9.2
G3	1008.3	990.6	1263.5	5.9	10.0
G4	1019.9	1022.3	1268.5	5.9	9.9
G5	981.9	983.6	1236.7	6.0	10.1
H1	989.7	932.5	1245.3	6.0	10.2
H2	1016.0	971.7	1267.9	5.1	8.6
H3	998.0	950.6	1257.8	6.1	10.4
H4	1022.5	971.3	1274.8	5.1	9.2
H5	991.2	940.4	1235.8	6.1	10.0
i1	1009.1	1027.0	1253.3	6.0	10.0
i2	1010.4	1019.5	1269.3	6.1	10.6
i3	1004.9	1035.1	1261.9	5.8	9.8

i4	1026.1	1061.6	1274.4	5.3	8.9
i5	978.7	1045.0	1248.2	6.1	10.5
J1	1006.7	972.0	1256.7	5.8	9.6
J2	1007.4	975.9	1265.3	5.6	9.5
J3	998.1	958.4	1262.4	6.2	10.7
J4	1020.8	947.5	1269.9	5.5	9.6
J5	991.4	980.3	1253.5	6.2	10.1
K1	1003.8	983.9	1256.6	6.0	9.7
K2	1002.7	1001.7	1261.6	5.9	10.0
K3	1014.7	1013.8	1269.3	5.9	10.4
K4	1018.4	973.6	1274.7	5.7	9.6
K5	1002.6	947.5	1256.0	5.7	9.7
L1	1012.1	965.3	1262.9	5.7	10.0
L2	999.9	957.4	1262.8	5.8	9.9
L3	1022.3	1027.8	1279.0	5.4	9.2
L4	997.9	982.0	1268.4	6.0	9.9
L5	1013.3	980.8	1258.1	5.8	9.8
M1	996.0	1173.3	1267.4	5.9	9.2
M2	1009.6	1162.3	1264.3	5.8	8.9
M3	1022.5	1200.1	1279.5	6.0	9.3
M4	1015.4	1176.7	1267.0	5.9	9.1
M5	953.7	1173.0	1262.2	5.9	9.2
N1	1006.7	946.3	1261.7	6.0	9.8
N2	1007.8	972.2	1265.8	5.8	10.1
N3	1011.4	1003.5	1265.9	5.8	9.9
N4	992.9	937.3	1258.6	5.7	9.7
N5	985.5	976.7	1262.0	5.3	8.9
O1 (Without Grid)	1008.9	982.5	1265.8	6.6	10.6
O2 (Without Grid)	1005.3	950.5	1271.6	5.9	10.1
O3 (Without Grid)	1018.7	977.6	1273.2	6.1	10.7
O4 (Without Grid)	997.6	952.1	1248.4	5.7	10.0

O5 (Without Grid)	1006.7	951.7	1263.3	5.3	9.0

Table IV: Results of tensile tests for specimens obtained from sheet metal JFE CA 1180 - 1.2 mm thick

4.- DISCUSSION

All the results obtained were statistically analyzed. In this sense, the first thing to do was to check that they respond to a normal distribution. Then, as an example, the normality test applied to Elongation under fracture load give the results in Figure 2:

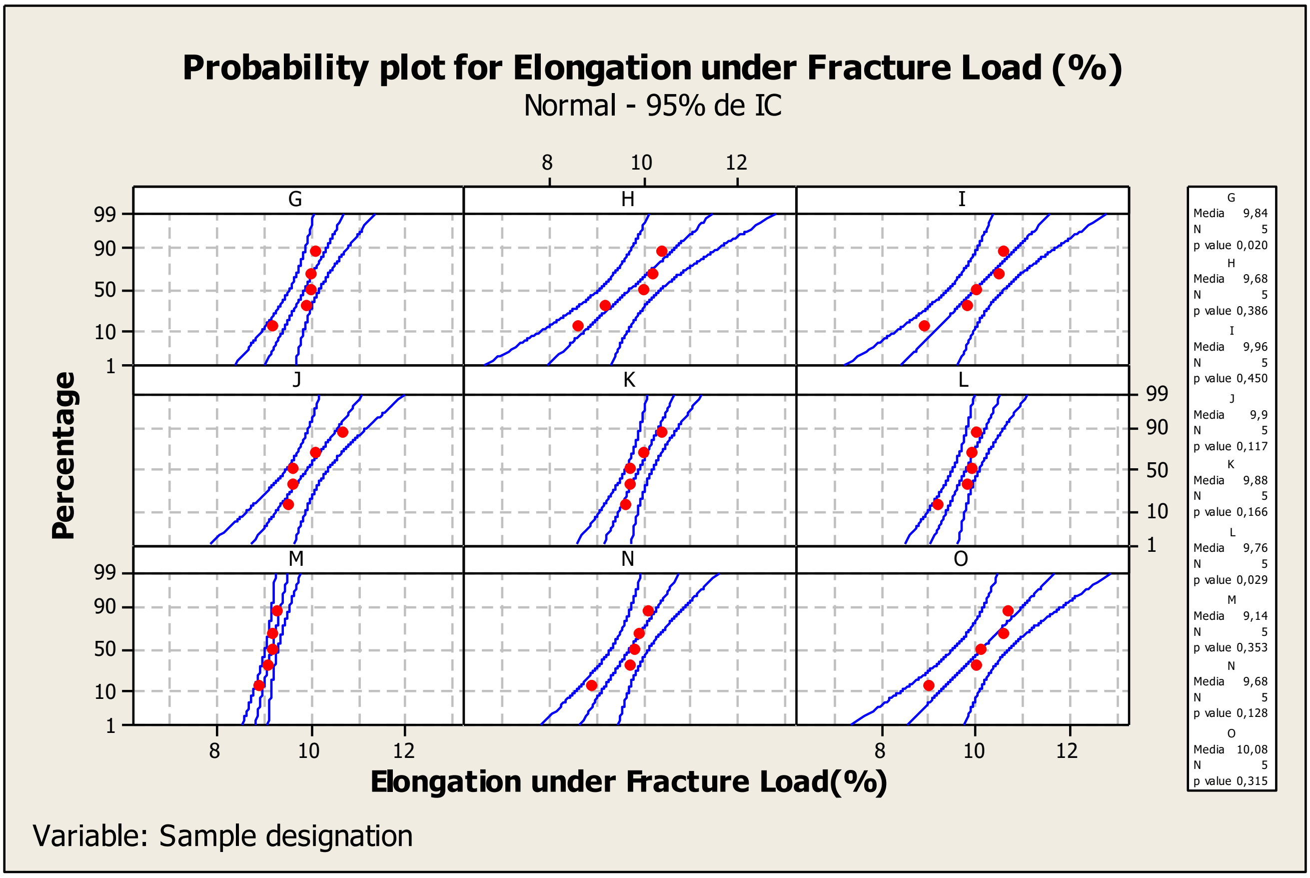

Figure 2: Probability plot for Elongation under fracture load below the eight engraving conditions

Here, straight blue lines represent the so-called fitted distribution line, whereas the curves correspond to the upper and lower bounds of the confidence interval. If the data distribution corresponds to an ideal normal, they should be on the fitted distribution line. Therefore, the results in Figure 2 indicate that, with the exception for combinations G and L, the rest of the engraving conditions evaluated, as regards Elongation under fracture load, the data respond to a normal distribution.

Another way to do a normality test is by using the p-statistic.

To analyze all the responses analyzed, the values of the p-statistic, obtained by means of variance analysis (ANOVA), are shown below for each response variable and grid laser marking condition:

Result	P values vs Grid laser marking condition							
	G	H	I	J	K	L	M	N
Yield Strength	0.521	0.260	0.290	0.692	0.074	0.469	0.168	0.259
Tensile Strength	0.517	0.830	0.806	0.866	0.438	0.316	0.110	0.356
Fracture Strength	0.321	0.356	0.831	0.483	0.874	0.196	0.145	0.666
Elongation under maximum load	0.580	**0.043**	0.230	0.600	0.109	0.543	0.165	0.363
Elongation under fracture load	**0.023**	0.318	0.425	0.123	0.134	**0.029**	0.214	0.091

Table V: Statistics p for the normality test

A p-statistic value greater than 0.05 indicates that data correspond to a normal distribution and can therefore be statistically analyzed. Note that of the forty combinations between response variables and grid laser marking conditions, only three of them cannot ensure 'normality' (see bold, table above).

Below are the box diagrams for the five response variables, in combination with the nine engraving conditions:

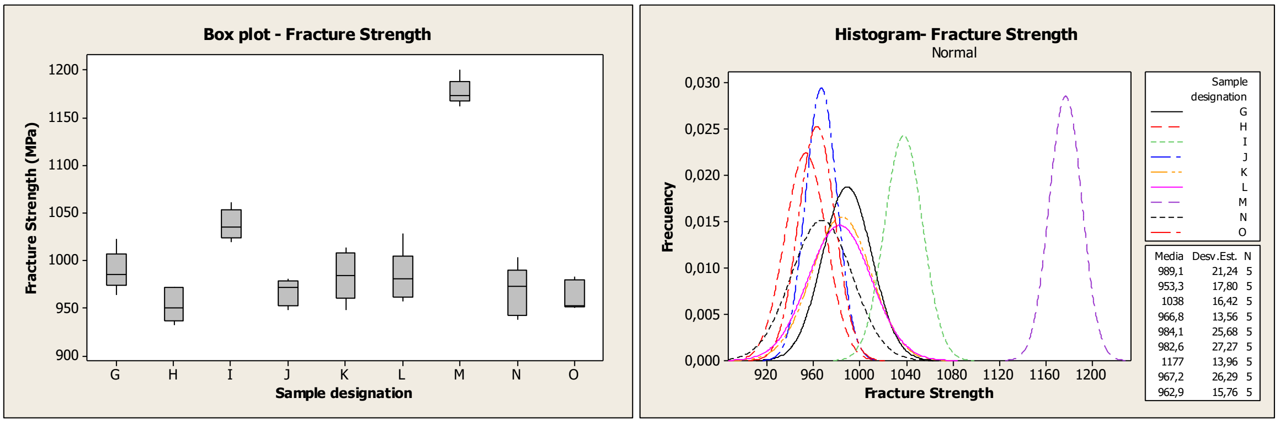

Figure 3: Diagram of boxes and histograms fracture strength

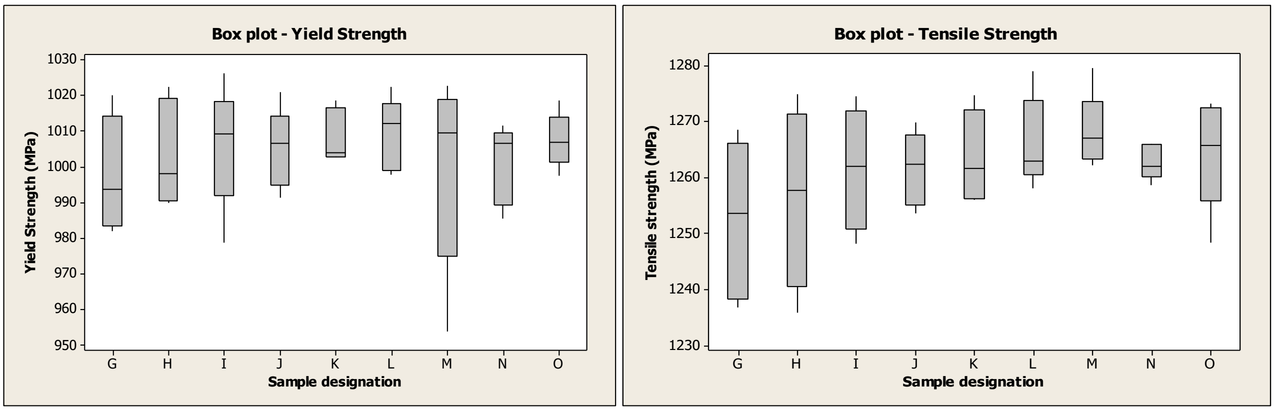

Figure 4: Box diagram for yield strength and tensile strength

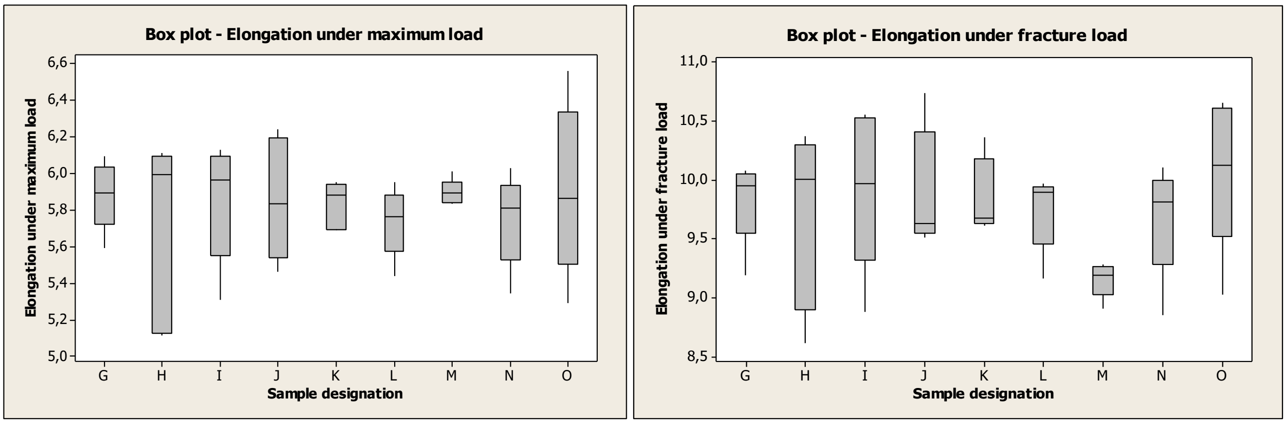

Figure 5: Box diagram for Elongation under maximum load and Elongation under fracture load

The boxes height is indicative of the dispersion of the results obtained. The average dispersion of the five mechanical properties analyzed, in the nine grid laser marking conditions, is in the range of 0.7 to 4.9%. According to Standard BS 10002-1, these percentages are adequate since in laboratory tests, the minimum accepted reproducibility is $\pm$ 5% for steel sheets.

With the results of the tensile tests, in order to compare the laser-engraved specimens with those that were not (named O), a balanced ANOVA analysis was performed for each response variable, considering the entire conditions (the eight grid laser marking and the no grid-shape), and the following p-statistics were obtained:

Response variable	Statistics p	Difference
Yield strength	0.927	Not significant
Tensile strength	0.338	Not significant
Fracture strength	0.000	Significant
Elongation under maximum load	0.947	Not significant
Elongation under fracture load	0.257	Not significant

Table VI: Values of the p statistic for the five responses obtained in the tensile tests (incidence of grid laser marking on each mechanical property)

A value for the $p > 0.05$ indicates that there are no significant differences between the groups, and that the analyzed mechanical properties have not been modified, when all engraving conditions are considered together. Meanwhile, as regards the fracture strength ($p = 0.000$), at least one of the groups produced significant differences from the rest. Looking at Figure 3 on the left it is apparent that this group is the M. Consideration is now given to the influence of each of the three engraving variables on the responses obtained from the tensile tests shown in Table VII:

Result	P values vs Laser engraving condition			
	Power	Focus	Number of passes	Result
Yield Strength	0,728	0,763	0,762	No significant influences
Tensile Strength	0,916	**0,025**	0,356	Focus significantly influences
Fracture Strength	**0,000**	**0,011**	**0,000**	They all have a significant impact
Elongation under maximum load	0,213	0,830	0,664	No significant influences
Elongation under fracture load	0,721	0,151	0,228	No significant influences

Table VII: Values of the p statistic for the five responses obtained in the tensile tests (incidence of the engraving variables on each mechanical property).

It arises from this analysis that the three operating variables of the laser, i.e. power, focus and number of passes, significantly influence the fracture strength, wherefore, the focus, does so on the tensile strength (see bold table above).

Through a complementary analysis with the Pareto tool of standardized effects, it was possible to establish that the most influential variable is the power, followed by the number of passes and finally the focus. The higher the power, the greater the number of passes and the smaller the focus size, the higher the fracture strength. Such is the case with condition M.

The stress - strain curves for specimens M, J, and O are shown below.

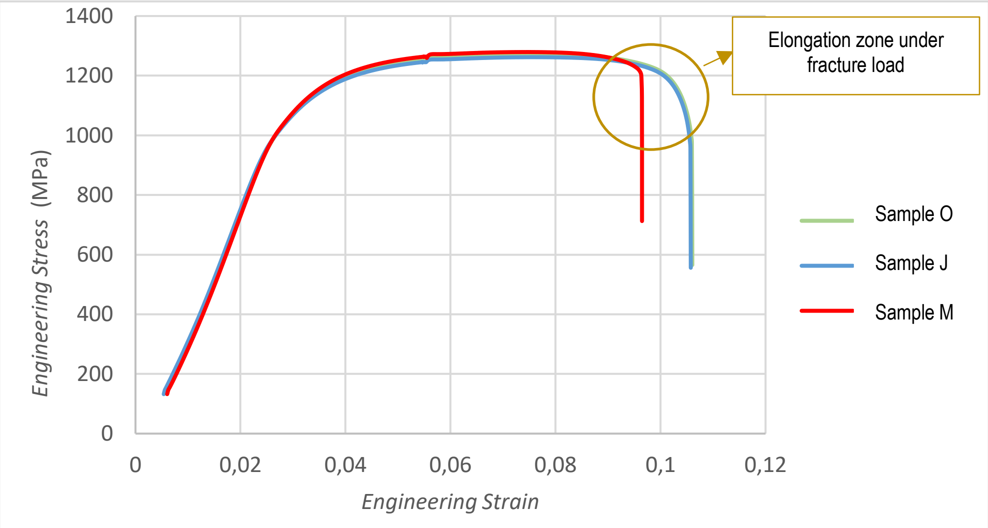

Figure 6: Stress - strain plot for O, J and M specimens

The diagrams in the figure above show a noticeable difference in the behavior of specimen M with respect to J and O in what makes the Elongation area under fracture load, observing an abrupt break in the M and more gradual in the J and O. Figure 7 shows a grid laser marking sector of a specimen engraved with condition M, where it is seen as the material, once tested to tensile, was cracked following the laser engraving own lines:

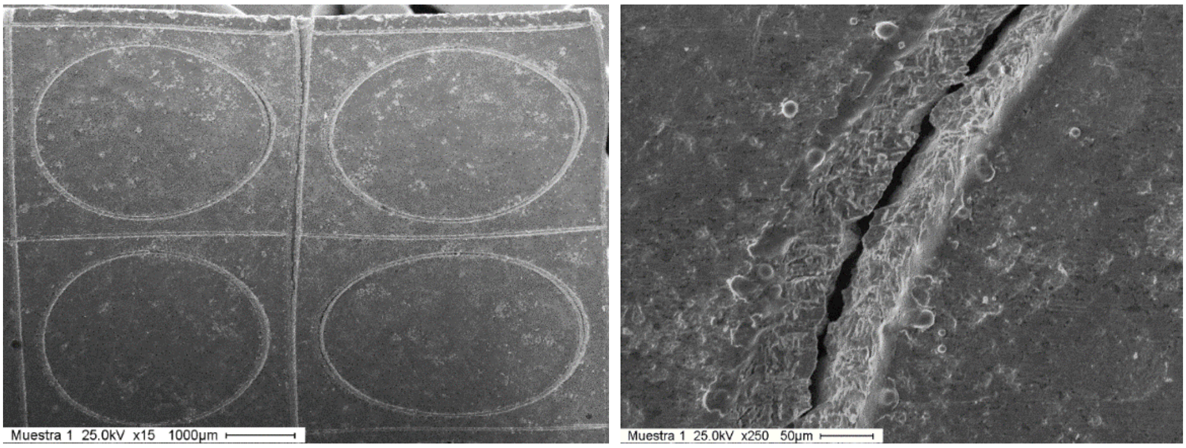

Figure 7: Sector of a tensile specimen tested, with grid in condition M (right) and crack detail

Another important aspect to consider of grid laser marking is visibility. This aspect, more subjective, and which turns out to be a function of the operational conditions of the laser (F = focus; Pa = number of passes and Po = percentage power), also depends on whether the visualization is done with the naked eye or under a microscope. This effect can be seen in Figure 8:

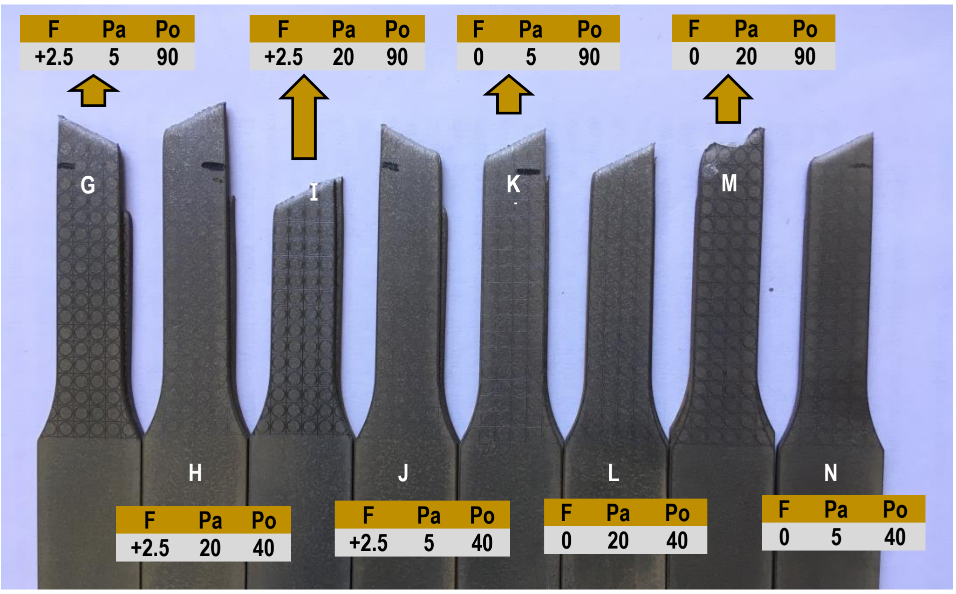

Figure 8: Viewing with the naked eye of grid laser marking obtained with the eight operating conditions of the laser

In particular, on the specimen engraved in condition M, fracture occurred following the grid engraving lines, and not at a characteristic angle, as it resulted in all other conditions.

The last aspect of being analyzed was the fracture of the specimens. By means of Figure 8, it is observed that fractures occurred approximately in the center of the calibrated length, with diagonal fracture in most cases, represented by a fracture angle of 64.6° ± 2.5°. This type of fracture, with minimal reduction of cross section area, is characteristic of high-strength steels [25].

5. CONCLUSIONS

Finally, by way of conclusions, it can be said:

- ✓ In this work, exclusively specimens were tested in JFE CA 1180. Consequently, laser engraving conditions cannot be extrapolated to different materials until other studies are carried out.
- ✓ Of the different laser variables, when they caused an affectation, were the percentage of power, the number of passes and the focus, and in that order, the variables with the greatest influence on mechanical properties.
- ✓ While increased power and the number of passes increase resistance, the focus to +2.5 mm decreases it.
- ✓ Under the specimen grid laser conditions designated as M (in focus, more passes and power), the fracture of the specimen occurred following the lines of the grid and this happened with the slightest Elongation under the fracture load (see Figure 6).
- ✓ It is apparent from all the studies carried out that the operating conditions of the laser, used for grid marking specimens designated as J, produced the slightest impact on mechanical properties, with visible grids, both with the naked eye and using optical microscope.

In the future, hot stamping will continue in use, and both simulation [6], the effects of production systems [12]-[23], increased use of tempered and polished laser [24], and lower costs, will be of interest.

References

[1]. Keeler S, Kimchi M, Mooney P. “Advanced High-Strength Steels Application Guidelines V6.0, April 2017, World Auto Steel

[2]. Huang M, Wang B, Zhou J, Li X. Investigation on mechanical properties distribution on hot stamped part. Procedia Engineering 81 (2014) 1774 – 1779. doi: 10.1016/j.proeng.2014.10.230

[3]. LN Lopez de Lacalle, A Lamikiz, J Muñoa, MA Salgado, JA Sánchez, Improving the high-speed finishing of forming tools for advanced high-strength steels (AHSS), The International Journal of Advanced Manufacturing Technology 29 (1-2), 2006, 49-63

[4]. Altan T, Tekkaya E, Sheet Metal Forming. Processes and applications. ASM International, 2012. ISBN-13: 978-1-61503-844-2

[5]. Ulintz P, Designing and Building Dies for High Strength Steel Stampings. March 2014. DOI: 10.4271/2014-01-0986

[6]. Fernández, B.; González, B.; Artola, G.; López de Lacalle, N.; Angulo, C. A Quick Cycle Time Sensitivity Analysis of Boron Steel Hot Stamping. Metals 2019, 9, 235

[7]. Mori K, Review of Shearing Processes of High Strength Steel Sheets. J. Manuf. Mater. Process. 2020, 4, 54; doi:10.3390/jmmp4020054

[8]. Naderi M, Ketabchi M, Abbasi M, Bleck W, Semi-hot Stamping as an Improved Process of Hot Stamping. J. Mater. Sci. Technol., 2011, 27(4), 369-376. DOI: 10.1016/S1005-0302(11)60076-5

[9]. Fernández B, González B, Artola G, López de Lacalle L.N, Angulo C, A Quick Cycle Time Sensitivity Analysis of Boron Steel Hot Stamping. Metals 2019, 9, 235; doi:10.3390/met9020235

[10]. Ortiz M, Penalva M, Iriondo E, López de Lacalle L.N, Accuracy and Surface Quality Improvements in the Manufacturing of Ti-6Al-4V Parts Using Hot Single Point Incremental Forming. Metals 2019, 9, 697; doi:10.3390/met9060697

[11]. Valoppi B, Sánchez Egea A, Zhang Z, González Rojas H, Ghiotti A, Bruschi S, Cao J, A hybrid mixed double-sided incremental forming method for forming Ti6Al4V alloy. April 2016. CIRP Annals - Manufacturing Technology. DOI: 10.1016/j.cirp.2016.04.135

[12]. Gonzalez-Ciordia, B.; Fernández, B.; Artola, G.; Muro, M.; Sanz, Á.; López de Lacalle, L.N. Failure-Analysis Based Redesign of Furnace Conveyor System Components: A Case Study. Metals 2019, 9, 816.

[13]. Bong H, Barlat F, Lee M, Ahn D, The forming limit diagram of ferritic stainless-steel sheets: Experiments and modeling. International Journal of Mechanical Sciences 64 (2012) 1–10. http://dx.doi.org/10.1016/j.ijmecsci.2012.08.009

[14]. Martínez Krahmer D, Polvorosa R, López de Lacalle L. N, Alonso-Pinillos U, Abate G, Riu F, Alternatives for Specimen Manufacturing in Tensile Testing of Steel Plates. Experimental Techniques, July 2016. DOI: 10.1007/s40799-016-0134-5

[15]. Schwindt C, Stout M, Iurman L, Signorelli J, Forming Limit Curve Determination of a DP-780 Steel Sheet. Procedia Materials Science 8 (2015) 978 – 985. doi: 10.1016/j.mspro.2015.04.159

[16]. Antúnez N, Martynenko V, Abate G, Perez D, Chiapparoli W, Martínez Krahmer D, Simulación computacional de un ensayo Erichsen aplicado a una chapa de acero DC-06. Revista Materia V23 N°2 (2018), Rio de Janeiro, Brasil. DOI: 10.1590/S1517-707620180002.0362

[17]. Ozturk F, Dilmec M, Turkoz M, Ece R, Halkaci H, Grid Marking and Measurement Methods for Sheet Metal Formability. 5th International Conference and Exhibition on Design and Production of Machines and dies/molds, June 2009, Aydin, Turkey.

[18]. Yildiz R, Yilmaz S, The verification of strains obtained by grid measurements using digital image processing for sheet metal formability. J Strain Analysis 2017, Vol. 52(8) 506–514 IMechE 2017. DOI: 10.1177/0309324717734669

[19]. Guk S, Plotnikova D, Kawalla R, The Effect of Microstructural and Geometric Inhomogeneities Induced by Laser for Forming Strain Analysis on Sheet Metal Formability. Materials Sciences and Applications, 2016, 7, 247-256, May 2016. http://dx.doi.org/10.4236/msa.2016.75025

[20]. Roy A, Kumar N, Das S, Bandyopadhyay A, Optimization of Pulsed Nd:YVO_4 Laser Marking of AISI 304 Stainless Steel Using Response Surface Methodology. Materials Today: Proceedings 5 (2018) 5244–5253. DOI: 10.1016/j.matpr.2017.12.107

[21]. Martynenko V, Szombach J, Perez D, Tilai Nieto D, Campana G, Martinez Krahmer D, Aplicación del microtexturado láser para la reducción del coeficiente de fricción en ensayos pin-on disk. VI Congreso Argentino de Ingeniería Mecánica, octubre 2018, Tucumán, Argentina

[22]. Martinez Krahmer D, Sánchez Egea A, Celentano D, Martynenko V, Cruchaga M, Friction characterization when combining laser surface texturing and graphite-based lubricants. December 2019, Journal of Materials Research and Technology. DOI: 10.1016/j.jmrt.2019.12.007

[23]. D Del Pozo, LNL de Lacalle, JM López, A Hernández, Prediction of press/die deformation for an accurate manufacturing of drawing dies. The International Journal of Advanced Manufacturing Technology 37 (7-8), 649-656

[24]. S Martínez, A Lamikiz, E Ukar, A Calleja, JA Arrizubieta, LNL de Lacalle, Analysis of the regimes in the scanner-based laser hardening process, Optics and Lasers in engineering 90, 72-80

[25]. C. Schwindt, Desarrollo experimental y modelado computacional multiescala de la curva límite de formabilidad. Aplicación a un acero dual-phase de alta Resistencia. Universidad Nacional del Sur, Bahía Blanca, Buenos Aires, Argentina, 2015 (Tésis de doctorado).

ACKNOWLEDGEMENTS

We would like to thank Mr. César Guereta, president of Sierra Technology, for facilitating the laser with which the grid laser marking of the tensile specimens were made, and Mercedes Pianetti from INTI-Mecánica to take the electronic microscope images.
Also, support for Basque Government University Groups IT1337-19, and minecor Challenges NewMine ministry project: RTC-2017-6039-5